Carbon monoxide hydrogenation on Fe_2O_3/ZrO_2 catalysts

Kaidong Chen, Yining Fan, Zheng Hu and Qijie Yan [1]

Department of Chemistry, Nanjing University, Nanjing 210093, PR China

Received 31 March 1995; accepted 22 September 1995

Fe_2O_3/ZrO_2 catalysts prepared by impregnation and coprecipitation methods were used for catalytic hydrogenation of CO. It was shown that the structure, reduction behavior of iron species, and catalytic properties of the catalysts were obviously affected by the preparation methods. For the Fe_2O_3/ZrO_2 catalyst prepared by the impregnation method, the Fischer–Tropsch catalytic activity and the selectivity to light olefins were much higher than those of the corresponding catalyst prepared by the coprecipitation method, the formation of methane was suppressed and the selectivity to light olefins was enhanced. Various intermediates formed during the successive steps of reduction of the catalysts were studied by using temperature-programmed reduction combined with in situ Mössbauer spectroscopy. The role of zirconia in the catalysts was discussed.

Keywords: CO hydrogenation; iron–zirconia catalyst; Mössbauer spectroscopy

1. Introduction

To meet the ever growing demand for chemical feedstocks, considerable attention has been paid to the design of Fischer–Tropsch (FT) synthesis catalysts with high selectivity to light olefins. In the past decade, iron catalysts promoted with transition metal oxides like MnO, TiO_2 and V_2O_5 have been extensively studied because of their high selectivity to olefins in CO hydrogenation [1]. The promoting effects of these additives have been discussed in detail [2–7].

Zirconia is currently attracting considerable scientific interest for its potential use as a catalyst support or promoter for a variety of catalyst systems [8]. It has been reported that zirconia can enhance the formation of alcohols when it is used as a support in CO hydrogenation catalysts. For example, zirconia-supported Cu catalysts exhibit both high activity and selectivity toward methanol synthesis [9,10]. Rh supported on zirconia favors the formation of ethanol [11]. Furthermore, zirconia itself can catalyze the CO hydrogenation reaction and produces isobutene very selectively at atmospheric pressure [12,13]. Recently, it has been reported that some metal-oxide catalysts promoted with zirconia can produce ethylene selectively [14]. Berry et al. [15] prepared iron–zirconia catalysts by the coprecipitation method and studied their catalytic properties for hydrogenation of CO; they found that the hydrocarbon product distribution for these catalysts showed Schulz–Flory α-values of 0.73–0.76. However, studies on zirconia used as a support or promoter to enhance the selectivity to light olefins in hydrogenation of CO were rather limited. The aim of this work is to study the behavior of Fe_2O_3/ZrO_2 catalysts for CO hydrogenation and to reveal the role of zirconia in the catalysts.

The structures, reduction behavior and catalytic properties of two 7 wt% Fe_2O_3/ZrO_2 catalysts prepared by different methods were studied by using XRD, XPS, TPR, Mössbauer spectroscopy and CO hydrogenation reaction test. It was found that the catalytic properties of the two catalysts were quite different. The Fe_2O_3/ZrO_2 catalyst prepared by the impregnation method showed high selectivity to light olefins.

2. Experimental

Fe_2O_3/ZrO_2 (A) and Fe_2O_3/ZrO_2 (B) catalysts were prepared by coprecipitation and impregnation, respectively. For the preparation of sample A, definite amounts of zirconium nitrate and iron nitrate were dissolved in deionized water and mixed thoroughly, 5 wt% ammonia solution was added dropwise to the above mixed solution with continuous stirring until the solution pH reached 7. The as-prepared precipitate was filtered and washed with water, then dried at 393 K for 24 h and calcined at 773 K for 5 h. For the preparation of sample B, zirconia (surface area 39 m^2/g, C.P. Shanghai) was impregnated with aqueous solution of iron nitrate, and then dried at 393 K and calcined at 773 K for 5 h.

X-ray diffraction measurements were performed on a Rigaku D/max-rA diffractometer using Cu Kα radiation. XPS measurements were performed in a V.G. ESCALAB MK II spectrometer. Binding energies were referenced to the C 1s peak at 285.0 eV. Mössbauer spectroscopy was conducted with a constant acceleration spectrometer using a 10 mCi $^{57}Co/Pd$ source. All spectra were computer fitted to a Lorentzian line shape with a least-squares fitting procedure, and the isomer shifts (IS) were given with respect to the centroid of α-Fe at room temperature. The TPR experiments were carried out in a U-type quartz reactor with heating rate of 16

---

[1] To whom correspondence should be addressed.

Table 1
CO hydrogenation on Fe_2O_3/ZrO_2 catalysts

Catalyst	CO conv. (%)	Hydrocarbon distribution (wt%)				
		C_1	C_2	C_3	C_4	$C^{=}_{2-4}/C^{0}_{2-4}$ (wt/wt)
ZrO_2	0.0					
A	1.1	100	–	–	–	–
B	6.4	37.5	33.2	22.8	6.5	2.1

K/min, and a flow rate of the H_2–Ar mixture (5.0 vol% hydrogen) of ca. 30 ml/min. Hydrogen consumption was monitored by a thermal conductivity detector. The as-prepared catalysts were located in a U-type quartz fixed bed microreactor and the catalytic properties were determined after the reaction reached steady state (ca. 12 h) with the reaction conditions at 643 K, 1 atm, $H_2/CO = 1.7$ (vol/vol) and GHSV ca. 600 h^{-1}. Reaction products were analyzed by an on-line gas chromatograph equipped with a Porapak-QS column and a thermal conductivity detector.

3. Results and discussion

3.1. CO hydrogenation

Table 1 shows the activity and selectivity of zirconia catalyst and Fe_2O_3/ZrO_2 catalysts for CO hydrogenation. For pure zirconia catalyst, under our reaction conditions no hydrocarbon product was detected, while the Fe_2O_3/ZrO_2 catalysts exhibited catalytic activity for FT synthesis. This indicated that iron species were the main active components in the Fe_2O_3/ZrO_2 catalysts. It was also pertinent to note that the catalytic activities and selectivities of these two Fe_2O_3/ZrO_2 catalysts were quite different. For sample A, the catalytic activity was very low, and almost 100% methane selectivity was observed. While for sample B, much higher catalytic activity was observed, a C_2–C_4 hydrocarbon selectivity of 62.5%, and $C_2^{=}$–$C_4^{=}/C_2^{0}$–C_4^{0} ratio of 2.1 was obtained. This reveals that for sample B the formation of methane was suppressed and the selectivity to light olefins was enhanced.

3.2. Structure of the catalysts

XRD, XPS, and Mössbauer spectroscopy were used for catalyst characterization. The Mössbauer parameters of the fresh catalysts are shown in table 2. For the sample A, X-ray diffraction lines of iron oxide were not observed. This indicated that iron-oxide particles were very small. The surface Fe/Zr atomic ratio measured by XPS was 0.11, which was quite close to the bulk Fe/Zr atomic ratio of 0.12, suggesting that the iron-oxide distribution is homogeneous both on the surface and in the bulk phase of zirconia. A doublet assigned to Fe^{3+} cations was observed in the Mössbauer spectra measured both at room temperature and 77 K (fig. 1); no sextet assigned to magnetic Fe_2O_3 was observed in the low temperature (77 K) spectrum. These results suggested that the Fe^{3+} cations existed in paramagnetic state. Accordingly, we may conclude that the Fe^{3+} cations have been incorporated into the lattice of zirconia and isolated during the process of preparation and existed as paramagnetic state. This conclusion is consistent with the results of Berry et al. [16] and Wold et al. [17]. They have reported that for the Fe_2O_3/ZrO_2 system Fe^{3+} cations could be randomly doped in the zirconia lattice in the process of preparation, hence the cubic zirconia could be stabilized at room temperature and the Fe^{3+} cations could exist in paramagnetic Fe_2O_3 state. For sample B, very weak X-ray diffraction lines of α-Fe_2O_3 were observed. Analysis by XPS showed 0.21 surface

Table 2
Mössbauer parameters of fresh Fe_2O_3/ZrO_2 catalysts at various temperatures

Catalyst	Temperature [a]	Mössbauer parameter			Iron species [b]	Relative area (%)
		IS (mm/s)	QS (mm/s)	*H* (kOe)		
A	RT	0.37	1.07	0	Fe_2O_3(P)	100
A	77 K	0.48	1.12	0	Fe_2O_3(P)	100
B	RT	0.43	−0.12	511	Fe_2O_3(M)	53
		0.35	1.03	0	Fe_2O_3(S)	47
B	77 K	0.47	−0.18	537	Fe_2O_3(M)	64
		0.40	1.05	0	Fe_2O_3(S)	36

[a] RT: room temperature.
[b] P: paramagnetic; M: magnetic, S: superparamagnetic.

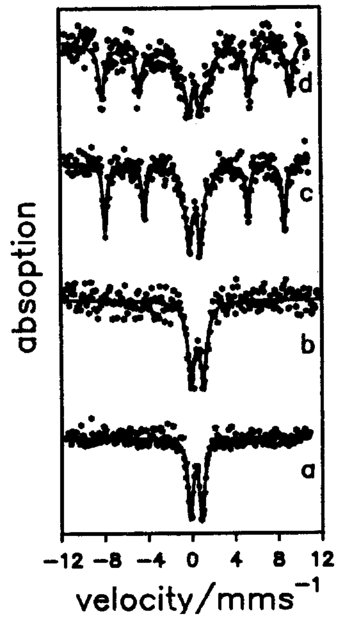

Fig. 1. Mössbauer spectra of fresh Fe_2O_3/ZrO_2 catalysts at various temperatures. (a) Sample A, measured at room temperature, (b) sample A, measured at 77 K, (c) sample B, measured at room temperature, (d) sample B, measured at 77 K.

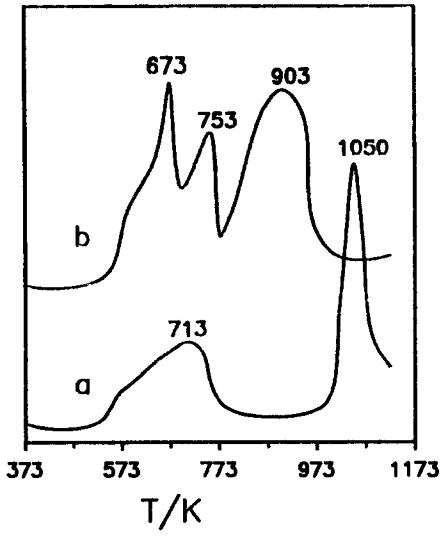

Fig. 2. TPR profiles of Fe_2O_3/ZrO_2 catalysts. (a) Sample A, (b) sample B.

Fe/Zr atomic ratio while the bulk Fe/Zr atomic ratio was 0.12. A sextet and a doublet assigned to magnetic and superparamagnetic α-Fe_2O_3 respectively were observed in the Mössbauer spectra (fig. 1). The average particle size of Fe_2O_3 calculated from the relative area of the sextet and the doublet was ca. 13.8 nm [18]. These results suggest that for the sample B, iron-oxide particles might be well dispersed on the surface of the support.

3.3. Reduction properties of the catalysts

TPR combined with in situ Mössbauer spectroscopy was used to study the reduction behavior of the two catalysts and the interactions between Fe_2O_3 and ZrO_2. TPR profiles of the two catalysts are shown in fig. 2. The reduction process of sample B mainly consisted of three consecutive stages with peak maximum at 673, 753 and 903 K respectively. For sample A, only two reduction stages with peak maximum at 713 and 1050 K were observed. Obviously, the different dispersion states of iron oxide for the two catalysts resulted in different interactions between Fe_2O_3 and ZrO_2, and hence influenced the reduction behavior of the catalysts. Various intermediates formed in the TPR process were identified by Mössbauer spectroscopy (table 3, figs. 3 and 4). For sample A, the two TPR peaks are considered to be corresponding to the following reduction stages:

$$Fe_2O_3 + H_2 \rightarrow FeO + H_2O$$

and

$$FeO + H_2 \rightarrow \alpha\text{-}Fe + H_2O$$

It has been reported [19] that bulk phase FeO is thermodynamically metastable compared with either magnetite or α-Fe at temperature below 840 K, thus wüstite can hardly be detected during the reduction of α-Fe_2O_3 to α-Fe. However, for Fe_2O_3/ZrO_2 catalyst prepared by the coprecipitation method, the Fe^{x+} ($x = 2$ or 3) cations are doped in the zirconia lattice, the interactions between them are very strong, and hence the FeO phase can be stabilized in the reduction process, making further reduction of the Fe^{2+} cations to Fe^0 very difficult.

For sample B, the first reduction stage is considered to be corresponding to

$$Fe_2O_3(m) + H_2 \rightarrow Fe_3O_4(m) + H_2O$$

$$ZrO_2 + H_2 \rightarrow ZrO_x\ (1.5 < x < 2) + H_2O$$

$$ZrO_x + Fe_3O_4 \rightarrow (Zr_yFe_{3-y})O_4$$

It is well known that zirconia is difficult to reduce, but partial reduction of the surface ZrO_2 to ZrO_x ($1.5 < x < 2$) is possible by thermal vacuum or hydrogen treatment, and Zr^{3+} ions were observed by ESR [20, 21]. Hence for the Fe_2O_3/ZrO_2 catalyst prepared by the impregnation method, although bulk phase zirconia cannot be reduced at 673 K, the iron cations might promote the reduction of the surface Zr^{4+} cations. Similar results were obtained by Borer et al. [22], who found that Ru could promote the reduction of zirconia at about 700 K. XPS results showed that the binding energy of Zr $3d_{5/2}$ shifted from 182.6 to 181.9 eV, which also seems to suggest that part of the surface Zr^{4+} cations were reduced to lower valence. Table 3 shows that the magnetic Fe_2O_3 was reduced to Fe_3O_4 in the first reduction stage. The ratio (S) of Mössbauer spectra area contributed by the iron cations in octahedral site to that of the tetrahedral site was observed to increase to a value of 3 compared to a value of 2 for bulk Fe_3O_4, indicating there were more iron cations in octahedral sites for the sample

Table 3
Mössbauer parameters of Fe_2O_3/ZrO_2 catalysts treated under various conditions

Sample	Treatment condition	Mössbauer parameter			Iron species	Relative area (%)
		IS (mm/s)	QS (mm/s)	H (kOe)		
A	as-prepared	0.37	1.07	0	Fe^{3+}	100
	TPR to 713 K	1.10	2.10	0	Fe^{2+}	100
	TPR to 1050 K	0.06	0.13	330	Fe^0	100
B	as-prepared	0.43	−0.12	511	Fe^{3+}	53
		0.35	1.03	0	Fe^{3+}	47
	TPR to 673 K	0.32	−0.07	490	Fe^{3+}	13
		0.77	0.00	467	Fe^{3+}, Fe^{2+}	40
		0.38	1.04	0	Fe^{3+}	47
	TPR to 753 K	1.06	0.00	0	Fe^{2+}	38
		0.46	1.01	0	Fe^{3+}	62
	TPR to 903 K	0.02	0.02	334	Fe^0	72
		0.38	0.99	0	Fe^{3+}	28

B than for pure Fe_3O_4. The only interpretation for this phenomenon is that the Zr^{2x+} ($1.5 < x < 2$) cations diffused into the tetrahedral sites of Fe_3O_4 and replaced part of the Fe^{3+} cations, showing a strong interaction between iron oxide and zirconia. These results are consistent with those reported by Gao et al. [23]. They found that for the Fe_2O_3/TiO_2 system, the Ti^{4+} cations could be reduced to lower valence in the reduction process and the iron cations in octahedral sites in the TiO_2-supported Fe_3O_4 were substituted by Ti^{x+} ($3 < x < 4$) cations from the support, resulting in the decrease of S.

The second reduction stage for sample B is considered to correspond to

$$(Zr_yFe_{3-y})O_4 + H_2 \rightarrow (ZrO_2)(FeO)_z + Fe_2O_3 + H_2O$$

During the second reduction stage, the inverse spinel structure of $(Zr_yFe_{3-y})O_4$ was destroyed, part of Fe^{3+} cations were reduced to Fe^{2+} cations and formed FeO which was doped by zirconium cations, hence the Fe^{2+} cations could be stabilized.

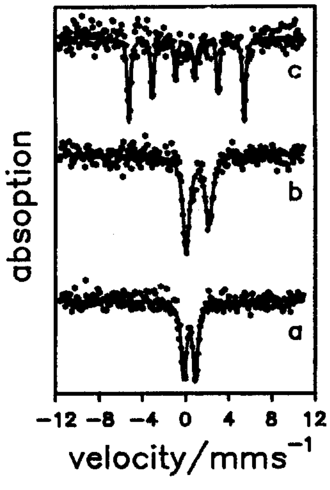

Fig. 3. Mössbauer spectra of Fe_2O_3/ZrO_2 catalyst A treated under various conditions. (a) As-prepared, (b) TPR to 713 K, (c) TPR to 1050 K.

The third reduction stage is considered to be corresponding to the reduction of

$$(ZrO_2)(FeO)_z + H_2 \rightarrow \alpha\text{-Fe} + ZrO_2 + H_2O$$

and

$$Fe_2O_3(s) + H_2 \rightarrow \alpha\text{-Fe} + H_2O$$

During the third reduction stage, the $(ZrO_2)(FeO)_z$ and part of the superparamagnetic α-Fe_2O_3 particles were reduced to α-Fe, while another part of the superparamagnetic Fe_2O_3 particles were not reduced due to their strong interactions with zirconia. From the above TPR results, it can be concluded that the iron species in sample A are more difficult to reduce to Fe^0.

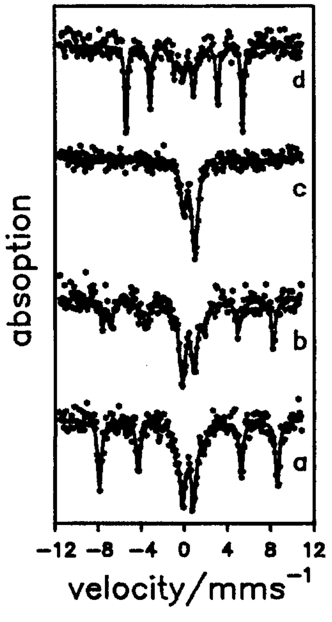

Fig. 4. Mössbauer spectra of Fe_2O_3/ZrO_2 catalyst B treated under various conditions. (a) As-prepared, (b) TPR to 673 K, (c) TPR to 753 K, (d) TPR to 903 K.

Table 4
Mössbauer parameters of Fe_2O_3/ZrO_2 catalysts in syngas atmosphere

Catalyst	Mössbauer parameter			Iron species	Relative area (%)
	IS (mm/s)	QS (mm/s)	H (kOe)		
A	1.07	2.33	0	FeO	100
B	0.33	1.12	0	Fe_2O_3	30
	0.34	0.00	220	χ-Fe_5C_2	70
	0.22	0.00	186		
	0.21	0.00	110		

3.4. Active phase of the catalysts

The in situ Mössbauer spectroscopic technique was also used to study the state of iron species in syngas atmosphere (fig. 5 and table 4).

For sample A, 100% FeO was observed from the Mössbauer spectrum. Thus under the reaction condition, Fe_2O_3 was reduced to FeO and stabilized; the FeO is thought to be the catalytic active phase. Since the dissociation of CO on iron oxide is rather difficult [24], and these Fe^{2+} cations were randomly doped in the zirconia lattice and isolated, the rather long distance between the active centers resulted in very difficult polymerization of the carbon-chain. This can account for the low catalytic activity and almost 100% methane selectivity for sample A. For sample B, the Mössbauer spectrum showed a superposition of iron carbide and high-spin Fe^{3+} cations correspond to 70% χ-Fe_5C_2 and 30% α-Fe_2O_3. Since α-Fe_2O_3 is not active for FT synthesis, we would suggest that the χ-Fe_5C_2 species is the catalytic active phase for sample B. According to the above TPR results, we assume that under the reaction conditions, the surface Zr^{4+} cations may also be reduced to lower valence and diffuse into the lattice of Fe_3O_4, forming $(ZrO_2)(FeO)_z$. Further reduction of $(ZrO_2)(FeO)_z$ in the syngas atmosphere will lead to the formation of highly dispersed Fe^0. Therefore the catalytic activity and the light olefins selectivity of sample B are much higher than that of sample A.

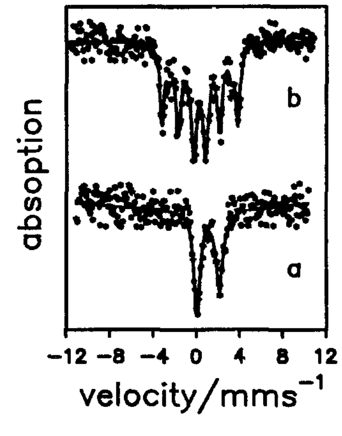

Fig. 5. Mössbauer spectra of Fe_2O_3/ZrO_2 catalysts in syngas atmosphere. (a) Sample A, (b) sample B.

4. Conclusion

The catalytic properties of 7 wt% Fe_2O_3/ZrO_2 catalysts were severely affected by the catalyst preparation method. For the sample prepared by the coprecipitation method, iron cations were doped in the lattice of zirconia and were difficult to reduce to Fe^0 because of its strong interaction with zirconia. This resulted in its lower catalytic activity and higher selectivity to methane. For the sample prepared by the impregnation method, iron cations can be easily reduced and carburized to highly dispersed χ-Fe_5C_2 in syngas atmosphere. The appropriate particle size of the active phase and the interactions between iron and zirconia suppressed methane formation and enhanced the selectivity to light olefins.

Acknowledgement

The support of the National Natural Science Foundation of China is gratefully acknowledged.

References

[1] M. Janardanro, Ind. Eng. Chem. Res. 29 (1990) 1735.

[2] J. Barrault and C. Renard, Appl. Catal. 14 (1985) 133.

[3] J. Barrault, C. Forquy and V. Perrichon, Appl. Catal. 5 (1983) 119.

[4] M.A. Vannice, J.Catal. 74 (1982) 199.

[5] H. Arai, K. Mitsuishi and T. Seiyama, Chem. Lett. (1984) 1291.

[6] U. Lochner, H. Papp and M. Baerns, Appl. Catal. 23 (1986) 339.

[7] B. Cornils, C.D. Frohning and K. Moraw, *Proc. 8th Int. Congr. on Catalysis*, Berlin 1984, Vol. 2 (Verlag Chemie, Weinheim, 1984) p. 23.

[8] A. Sofianos, Catal. Today 15 (1992) 149.

[9] B. Denise, R.P.A. Sneeden, B. Beuuin et al., Appl. Catal. 30 (1987) 353.

[10] B. Denise and R.P.A. Sneeden, Appl. Catal. 28 (1986) 235.

[11] M. Ichikawa, J. Chem. Soc. Chem Commun. (1978) 566.

[12] K. Maruya, T. Maehashi, T. Haraoka et al., Bull. Chem. Soc. Jpn. 61 (1988) 667.

[13] T. Maehashi, K. Maruya, K. Domen et al., Chem. Lett. (1984) 747.

[14] Su Guiqin, Zhang Wenzhong, Gao Runxong et al., KeXue TongBao (China) 13 (1991) 1038.

[15] F.J. Berry, S. Jobsen and M.R. Smith, Hyperfine Interactions 46 (1989) 607.

[16] F.J. Berry, M.H. Loretto and M.R. Smith, J. Solid. State Chem. 83 (1989) 91.
[17] S. Davison, R. Kershaw, A. Wold et al., J. Solid. State Chem. 73 (1988) 47.
[18] W. Kündlg, H. Bömmel, G. Constabaris et al., Phys. Rev. 142 (1966) 327.
[19] A.J.H.M. Koch, H.M. Fortuin and J.W. Geos, J. Catal. 96 (1985) 261.
[20] C. Morterra, E. Giamello, L. Orio et al., J. Phys. Chem. 94 (1990) 3111.
[21] M. Anpo, T. Nomura, J. Kondo et al., Res. Chem. Intermed. 13 (1990) 195.
[22] A.L. Borer, C. Bronnimann and R. Prins, J. Catal. 145 (1994) 516.
[23] X. Gao, J. Shen, Y. Hsia et al., J. Chem. Soc. Faraday Trans. 89 (1993) 1079.
[24] J.E. Kubsh, Chen Yi and J.A. Dumesic, J. Catal. 71 (1981) 192.